CONTROLLED EXCITATION OF SCAR MODES IN PASSIVE AND ACTIVE MULTIMODE CHAOTIC FIBERS

Claire Michel, Valérie Doya, Sorin Tascu, Wilfried Blanc, Olivier Legrand, Fabrice Mortessagne

CONTROLLED EXCITATION OF SCAR MODES IN PASSIVE AND ACTIVE MULTIMODE CHAOTIC FIBERS

Claire Michel, Valérie Doya*, Sorin Tascu, Wilfried Blanc, Olivier Legrand, Fabrice Mortessagne

Université de Nice Sophia-Antipolis
Laboratoire de Physique de la Matière Condensée, CNRS UMR 6622
06108 Nice, France

**Corresponding author: valerie.doya@unice.fr*

A multimode optical fiber with a D-shaped cross section is an experimental paradigm of a wave system with chaotic rays' dynamics. We show that seldom but usable modes, called scar modes, localized along some particular direction of the geometrical trajectories can be selectively excited. We report numerical simulations that demonstrate the importance of the so-called self focal point in the scar modes selection process. We use a localized illumination in a passive fiber, or, a localized gain in an Ytterbium-doped fiber, located in the vicinity of this special point to control the scar modes selection.

OCIS codes: 350.5500, 060.2320.

1. Introduction

The behavior of waves in a 2-dimensional bounded domain (billiard) is determined by the nature of the rays' dynamics in the geometrical limit. For simple shapes as the circle or the square, the rays' dynamics is regular but tends to be complex as the shape becomes more complicated. When the rays' dynamics presents the property of high sensitivity to initial conditions, the dynamics is chaotic. The influence of the chaotic nature of the dynamics on the properties of waves constitutes the active field of investigations of Wave Chaos [1]. From vibrating plates [2], to microwave cavities [3, 4] or optical fiber [5], all these various systems present generic features well-described by theoretical predictions that demonstrate the universality of Wave Chaos.

Investigating how the chaotic geometrical limit influences the wave properties is not only a fundamental issue but reveals also applications in various domains ranging from room acoustics to reverberant electromagnetic cavities. Optics in particular is getting advantages of wave chaos. Chaotic fibers [6] are used to optimize the pump power absorption in double clad fiber amplifier and chaotic shapes provide improved features to microlasers [7–9].

As mentionned above, a multimode optical fiber with a truncated (D-shaped) cross section (see fig. 1) and large dimensions compared to the wavelength has been proved to be an efficient experimental tool to investigate the spatial properties of waves that propagate in a chaotic system [5]. Indeed, as the optical fiber is invariant along the direction of propagation z, the projection of the z-evolution of a ray over its transverse cross section can be seen as the time-evolution of a ray in the D-shaped billiard (see fig. 1(b)). The chaotic nature of the rays' dynamics in the D-shaped billiard controls the properties of the propagating modes in the wave-analogous system.

Generic modes of chaotic systems are ergodic modes: their intensity is statistically uniformly distributed all over the cross section (fig. 1(c)). This behavior is the result of multiple interferences encountered by the waves that reflect on the chaotic boundary [10]. Nevertheless, some surprising modes may appear: they present strong localization of intensity along the direction of some periodic trajectories of the associated billiard. For these non-ergodic modes, called scars [11], the spreading of intensity is "frozen" by constructive interferences along a periodic orbit. The intensity of the field of different scar modes along the short 2-bounce periodic orbit (p.o.) is presented in fig. 2. These singular modes have been the object of numerous theoretical investigations [12–14] and, recently, have been used in the field of applied optics. Their localized enhancement of intensity offers interesting properties: scar modes are currently employed in microlaser cavities to increase the directivity of laser emission and decrease the laser threshold [7–9].

These scar modes reveal some signatures of the underlying geometrical limit. They mark some periodic trajectory and concentrate their intensity over a specific point. In this paper, we utilize this "geometrical point" to excite selectively the scar modes which are difficult to exhibit in a multimode fiber. We show that in a passive multimode fiber, a localized excitation can select some scar modes. In order to be less dependent on the illumination condition, we propose, in a second part, to perform a "scar mode amplifier" by introducing a localized gain to control wave chaos. The conclusive part of the present paper is dedicated to the description of experimental feasibility of the scar modes amplifier.

2. Scar selection by localized excitation

The system we use is a silica fibre with n_{core}=1.451 surrounded by a low refractive index silicone cladding with $n_{cladding}$=1.41. The fibre is truncated at half its radius R=60μm. Scar

modes can exist along a periodic orbit if $\mu\mathcal{L} << 2\pi$ where μ is the Lyapunov coefficient (i.e. the rate of divergence of two close initial conditions measured in the phase space) and $\mathcal{L}$ the length of the orbit. When this condition is fulfilled, constructive interferences along the periodic orbit freeze the development of the chaotic dynamics leading to localized scar modes. We consider the 2-bounce p.o. which is the shortest periodic orbit of the D-shaped billiard, with $\mathcal{L} = 3R$ and $\mu = 0.4/R$, so that scar modes along the 2-bounce p.o. can exist. The condition of constructive interferences along the 2-bounce p.o. defines the transverse wavenumber κ_p associated to a scar mode of order p (fig. 2(a)-(f)):

$$\kappa_p\mathcal{L} - \Delta\varphi - \frac{\pi}{2} = 2\pi p \tag{1}$$

$\Delta\varphi$ is the phaseshift induced by the reflection at the core/cladding interface that depends on κ_p, n_{core} and $n_{cladding}$ and p is an integer. The additional $\pi/2$ phaseshift is due to the unique self-focal point [15] on the 2-bounce p.o. A pencil of rays emitted from a self-focal point will focus on this same point after one period. Moreover, we note that the D-shaped cross section mimicks an unstable Fabry-Perot resonator: the self-focal point is close to the focal point of the curved dielectric mirror.

This special point concentrates rays and also corresponds to a maximum of intensity for the scars that can be exploited for selective excitation. As seen in fig. 2, most of the scar modes along the 2-bounce p.o. exhibit a maximum of intensity in the vicinity of the self-focal point. This distinctive feature gives rise to the technique that we propose for achieving a selective excitation of scar modes: use an initial illumination with a Gaussian shape centered on this intensity spot. At the input of the fiber, the field of the Gaussian beam is decomposed over a finite number of guided modes whose weights are given by their spatial overlap with the incoming light. In order to preferentially excite the scar modes, the width of the Gaussian is set to the mean diameter of the bright spot which characterizes these modes, in practice $\sigma = 5.64\,\mu$m. To describe the spectral contents of the field evolving along the fiber, we introduce the $\kappa - z$-spectrum $C(\kappa, z)$ defined as the Fourier transform of the correlation function of the field $\psi(\vec{r})$ with its initial condition [16, 17]:

$$C(\kappa, z) = \int_{z-(L_z/2)}^{z+(L_z/2)} dz' \int\int d\vec{r}\psi^*(\vec{r}, 0)\psi(\vec{r}, z')e^{-i\beta(\kappa)z'} \tag{2}$$

where β is the longitudinal wavenumber and L_z a propagation length. We use an algorithm implementing the Beam Propagation Method to simulate the propagation of the initial field along the fiber [5,18]. The figure 3(a) shows the $\kappa-z$-spectrum calculated after a propagation length that ensures that all the modes are well established. This figure has to be compared to the calculated spatial overlap between the initial Gaussian beam and the scar modes shown in fig. 3(b).

We note that only a few modes dominate the spectrum: the scar modes from order 1 to 5. The

excited modes correspond to the one having a maximal spatial overlap with the Gaussian input field. Thus, as the Gaussian beam is launched on the high intensity area of the scar modes, its spatial overlap is larger for scar modes than for the generic speckle modes.
In a "passive" multimode chaotic fiber, we use the complex spatial structure of the modes to select some of them. One stigma of the geometrical dynamics, the self-focal point, arises in the spatial distribution of intensity of the scar modes and can be exploited to control the selection of scar modes. A perfect localization of excitation on the self-focal point can act as a scar modes selector but this method relies on a perfect command on the location and characteristic of the initial beam.

3. Scar selection using gain

The challenge is to overcome the intrinsic limitation of a passive system by introducing an active medium inside the fiber. The main question is: how to determine the optimized distribution of the gain ? A hint to answer may be found in a closely related domain. Indeed, some recent investigations in disordered media with gain have shown that a given localized mode can be selectively excited through a pumping confined to its spatial extension [19]. In our case, due to technical constraints, there is no hope that the active medium precisely match the spatial pattern of a given scar mode. But here again the high intensity area close to the self-focal point will be helpful: we consider an Ytterbium-doped multimode fiber with the gain region localized on the position of the bright spot. To prevent light from being guided in the doped area, we consider a small but realistic refractive index difference between the silica core and the doped area of 5.10^{-4}. To pump the system, a laser at 980 nm is focused in the large chaotic truncated core. The large number of ergodic modes excited ensures an uniform absorption of the pump along the propagation [20, 21]. The field of the pump is absorbed by the active ions and acts as a power reservoir for the signal. In order to evaluate the efficiency of the modes selection by the localized gain, a spatially incoherent signal (speckle field) at 1064 nm is coupled into the D-shaped core. The initial coupled energy is therefore spread over a great number of modes.
In figure 4(a), we report the far-field intensity of the signal at the input of the fiber integrated over the radial coordinate ϕ_κ, $\widetilde{I}(\phi_\kappa)$. The inset presents the initial far-field intensity $\widetilde{I}(r_\kappa, \phi_\kappa)$. All the wavenumber directions are explored. We let the field evolve along the fiber: amplification occurs and after 40 m of propagation along the exotic fiber amplifier, the maximum amplification factor is achieved. We note z_{max} this length of maximum amplification. We plot the same quantities as (fig. 4(a)) in (fig. 4(b)) for $z = z_{max}$. We can observe that a strong transverse wavenumber filtering process occurs during the propagation. The integrated far-field intensity tends to concentrate over two privileged angles that correspond to values of ϕ_κ equal to $\pi/2$ and $3\pi/2$. These angles are associated to the direction of the trans-

verse wavenumber of the waves that bounces back along the direction of the 2-bounce p.o. In the far-field pattern, we can also notice that some peaks concentrate the intensity along the 2-bounce p.o. exhibiting a selection on the transverse wavenumber not only on direction but also on the modulus. With the aim to get more informations on the mode selection process induced by the gain, we analyze the transverse wavenumber spectrum calculated for the length z_{max}. We notice that few selected modes appear in the wavenumber spectrum: only some modes get amplified along the propagation.

In table 6, the theoretical values of the scar mode wavenumbers deduced from Eq. (1) are compared to the wavenumbers corresponding to the peaks in the numerical spectrum. The comparison clearly establishes that each amplified wavenumber is associated to a scar mode wavenumber. This result and the particular structure of the far-field pattern shown in fig. 4(b) conspire to demonstrate that the amplification mechanism applies only to the scar modes. From the spatial overlap of a given scar mode with the doped region, one can even obtain its amplification rate thus accounting for the relative amplitudes of the different amplified scar modes. The diamonds in fig. 5 show the values taken by these overlaps. They are compared to the amplification rates directly deduced from the evolutions of the scar mode powers. The typical evolution of the power along the fiber is exemplified in fig. 6 for the scar mode of order $p = 4$. In a semi-logarithmic scale, the power exhibits a linear growth before reaching a plateau which corresponds to the saturation of the amplification mechanism. The amplification rate is then obtained through a linear fitting procedure by assuming a uniform amplification process of the form:

$$P_p(z) = P_p(0)\exp(\alpha_p z), \tag{3}$$

The constant slope of the curve gives the amplification rate α_p. The crosses in fig. 5 represent the values of α_p for the different scar mode orders. The good agreement between the two quantities emphasizes the importance of the overlap of the field with the doped area on the differential modes amplification process. The location of the gain controls the scar mode amplification: to get an efficient amplification, the doped area should have a good interaction with the scar modes.

4. First step to experimental realization

The experimental investigation of the selective amplification process put numerically into evidence requires the realization of a non-conventional fiber amplifier. This has been achieved and the experiments is under progress. In a first step, we performed a silica preform doped with 1250 ppm of Ytterbium ions by means of a standard MCVD (Modified Chemical Vapor Deposition) method. Ytterbium ions are incorporated without other ions as Aluminium usually used to ensure a good incorporation of rare-earth ions in the silica matrix. The index

profile measured on the preform confirms the presence of Ytterbium ions by the way of a refractive index increase of 5.10^{-4}. Due to this small refractive index difference between the doped area and the core, the fundamental mode of the weakly guiding doped area is spatially extended and suffers from important losses. As a consequence, this mode is not supported along the propagation. The MCVD method imposes the active ions to be located in the center of the preform. In order to localize the doped area in the vicinity of the self-focal point and also to get a D-shaped silica core, the circular preform is machined: a smaller preform with an off-centered doped area is cut into the preform [22]. Then, the preform is pulled by controlling the temperature and the drawing velocity to get the fiber with a well-preserved D-shaped geometry and diameter over hundred of meters. We use a low refractive index polymer (Luvantix UVF PV-409R04AP) as the optical cladding. The figure 7 is the absorption spectrum of the Ytterbium-doped fiber measured experimentally. The general behavior corresponds to the generic absorption spectrum of Ytterbium in silica matrix. From this measure, we can deduce an estimation of the absorption coefficient at the pump wavelength, $a_p = 6.2$dB/m.

To perform the scar mode amplifier, we realize the following experimental setup. A pump laser diode at 978 nm is focused at the fiber input. The signal from a Yag laser at 1064 nm is collimated and launched at the fiber input. A dichroic mirror is used to couple both the signal and the pump at the fiber input. For the signal illumination, we can either used a focused beam or a diffuse beam (for a noisy field illumination). We depict in the figure 8 the evolution of the gain curve along the propagation. The gain is obtained from the measured signal at the fiber output in presence of the pump over the measured signal without pump. The curve increases up to a critical length $z_{max} \simeq 15\,m$ associated to the saturation length of the signal. We note that the value of the gain is small compared to usual optical amplifier. Indeed, this amplifier is unusual from different aspects: as instance, the quantity of incorporated Ytterbium is small (and without aluminium co-doping) and the signal propagates in a large D-shaped core reducing the interaction with the doped area is reduced. Nevertheless, the gain curve clearly shows that an amplification process occurs along the propagation: optical amplification is achieved with this exotic active fiber. The next step is to control the initial illumination so that the amplification occurs on the scar modes. This step is under process and will constitute the purpose of a forthcoming publication.

5. Conclusion

In systems that exhibiting deterministic chaotic in the geometrical limit, some modes show surprising enhancement of intensity along geometrical periodic orbit of the corresponding billiard. These modes are of particular interest because they freeze the chaotic nature of the system and tend to concentrate intensity in finite regions of the system. Nevertheless,

they are isolated and sparse modes. We demonstrate that the self-focal point proper to the 2-bounce periodic orbit can be used to select the scar modes in a billard-analogous wave system: a D-shaped optical fiber. Intensity of the scar modes is concentrated on the self-focal point: we prove that using a localized excitation in a passive fiber, or introducing a localized gain on this specific point, we can excite selectively the scar modes. Thus, a pure geometrical quantity, the self-focal point, may play a crucial role on the wave properties. These numerical investigations have been done using realistic datas from measurements and the experiment of scar amplifier is currently in progress.

6. Acknowledgement

We want to address grateful thanks to S. Trezien and M. Udé for their technical supports in the preform and fiber manufacture. We also acknowledge fruitful discussion with P. Aschieri. This work is part of the projet n^o 05-JCJC-0099-01 supported by the Agence Nationale de la Recherche.

References

1. H.-J. Stöckmann, *Quantum Chaos: an introduction* (Cambridge University Press 1999).
2. K. Schaadt, T. Guhr, C. Ellegaard, M. Oxborrow, " Experiments on elastomechanical wave functions in chaotic plates and their statistical features", Phys. Rev. E **68**, 036205 (2003).
3. H.-J. Stöckmann, J. Stein, ""Quantum Chaos" in billiard studied by microwave absorption", Phys. Rev. Lett. **64**, 2215-2218 (1990).
4. S. Sridhar, "Experimental observation of scarred eigenfunctions of chaotic microwave cavities", Phys. Rev. Lett. **67**, 785-788 (1991).
5. V. Doya, O. Legrand, F. Mortessagne, and Ch. Miniatura, "Speckle statistics in a chaotic multimode fiber", Phys. Rev. E **65**, 050223 (2002).
6. V. Doya, O. Legrand, and F. Mortessagne, "Optimized absorption in a chaotic double-clad fiber amplifier", Opt. Lett. **26**, 872-874 (2001).
7. T. Harayama, T. Fukushima, P. Davis, P. O. Vaccaro, T. Miyasaka, T. Nishimura and T. Aida, "Lasing on scar modes in fully chaotic microcavities", Phys. Rev. E **67**, 015207 (2003).
8. W. Fang and H. Cao, "Wave interference effect on polymer microstadium laser", Appl. Phys. Lett. **91**, 041108(2007).
9. W. Fang, A. Yamilov, and H. Cao, " Analysis of high-quality modes in open chaotic microcavities", Phys. Rev. A **72**, 023815 (2005).
10. M. V. Berry, "Regular and irregular semiclassical wavefunctions", J. Phys. A: Math. Gen. **10**, 2083, (1977).

11. E. J. Heller, "Bound-State Eigenfunctions of Classically Chaotic Hamiltonian Systems: Scars of Periodic Orbits", Phys. Rev. Lett. **53**, 1515, (1984).
12. M. V. Berry, "Quantum scars of classical closed orbits in phase space", Proc. R. Soc. Lond. A **423**, 219-231 (1989).
13. L. Kaplan, "Scars in quantum chaotic wavefunctions", Nonlinearity **12**, R1-R40 (1999).
14. B. Li, "Numerical study of scars in a chaotic billiard", Phys. Rev. E **55**, 5376-5379 (1997).
15. E. B. Bogomolny, "Smoothed wave functions of chaotic quantum systems", Physica D **31**, 169-189 (1988).
16. M.D. Feit and J. A. Fleck, Jr, "Computation of mode properties in optical fiber waveguides by a propagating beam method", Appl. Opt. **19**, Issue 7, 1154-1164 (1980).
17. C. Michel, V. Doya, O. Legrand and F. Mortessagne, "Selective Amplification of Scars in a Chaotic Optical Fiber", Phys. Rev. Lett. **99**, 224101 (2007).
18. M.D. Feit and J. A. Fleck, Jr, "Light propagation in graded-index optical fibers", Appl. Opt. **17**, 3990-3998 (1978).
19. P. Sebbah and C. Vanneste,"Random laser in the localized regime" Phys. Rev. B **66**, 144202 (2002).
20. V. Doya, O. Legrand, and F. Mortessagne, "Optimized absorption in a chaotic double-clad fiber amplifier", Opt. Lett. **2**6, 872 (2001).
21. P.Leproux, V.Doya, P.Roy, D.Pagnoux, F.Mortessagne, O.Legrand, "Experimental study of pump power absorption along rare-earth-doped double clad optical fibres", Opt. Commun. **218**, pp. 249-254 (2003)
22. This step has been realized in collaboration with the Optical Development Workshop in the Institute of Plasma Physics, Prague, Czech Republic.

Table caption

Tab1 The table reports the theoretical value of the transverse wavenumber for each scar mode of order p along the 2-bounce p.o. compared to the measured value of the transverse wavenumber associated to the peak (amplified modes) on the spectrum.tab1.ps

Figure Captions

Fig1 Transverse cross section of the D-shaped multimode fiber (a), typical rays' trajectory in the associated D-shaped billiard (b) and generic speckle mode of a D-shaped chaotic optical fiber (c).fig1.eps

Fig2 Scar modes along the 2-bounce periodic orbit. The integer p labels the order of the scar mode. fig2.eps

Fig3 Transverse wavenumber spectrum (a) for a gaussian beam excitation. Spatial overlap between the gaussian beam and the modes(b). In both figures, the number on each peak labels the order of the scar mode. The first peak corresponds to the fundamental mode. Spectrumgauss3.eps,Recouvgauss3.eps

Fig4 Radial integrated far-field at the fiber input(a) and the maximum amplification length(b). The inset shows the whole far-field pattern.fig4.eps

Fig5 Overlap of the field of each scar mode with the doped area (square) compared to the amplification coefficient (cross).fig5.eps

Fig6 Exponential evolution of the power associated to the scar of order 4.fig6.eps

Fig7 Absorption spectrum measured in the fiber.fig7.eps

Fig8 Experimental measure of the gain in the Ytterbium doped D-shaped fiber with an off-centered core.fig8.eps

TABLE 1

p	κ_p from eq.1	measured κ_p
1	4.69	4.70
2	6.78	7.06
3	8.86	9.05
4	10.95	10.99
5	13.03	13.10
6	15.12	15.29
7	17.20	17.23
8	19.29	19.59
9	21.37	21.53
10	23.46	23.68
11	25.02	25.80
12	27.10	27.93
13	29.19	29.80

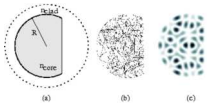

FIGURE 1

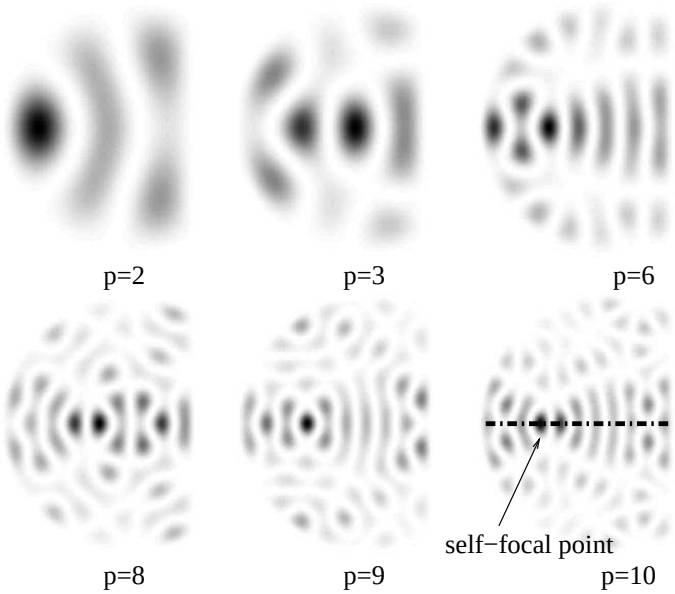

FIGURE 2

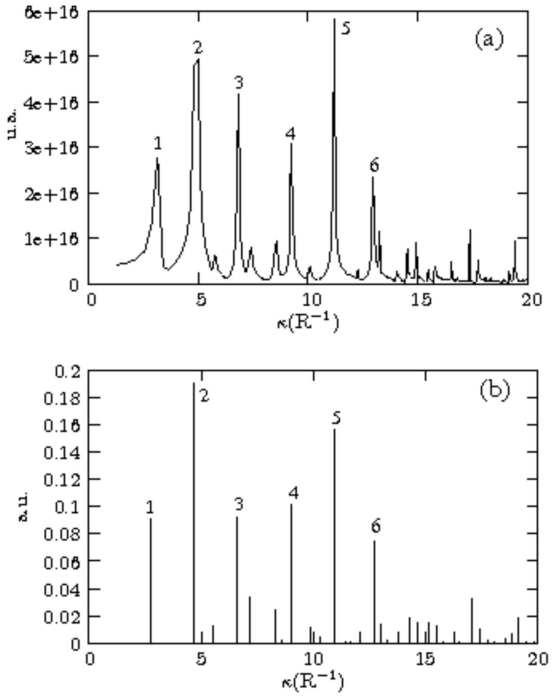

FIGURE 3

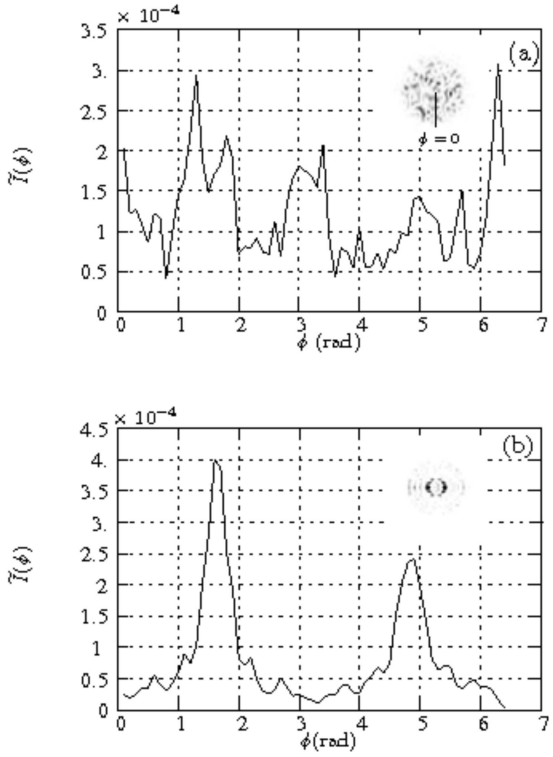

FIGURE 4

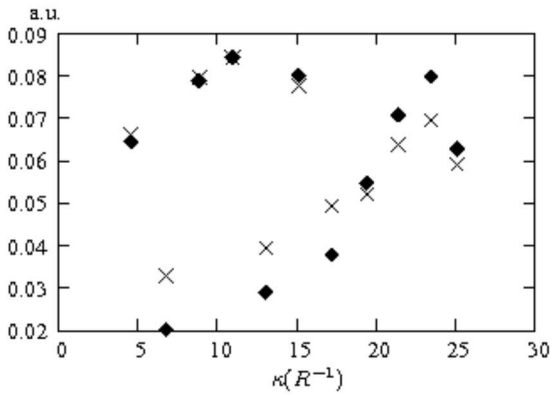

FIGURE 5

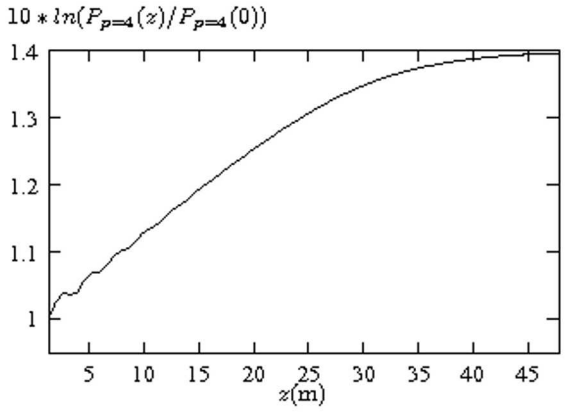

FIGURE 6

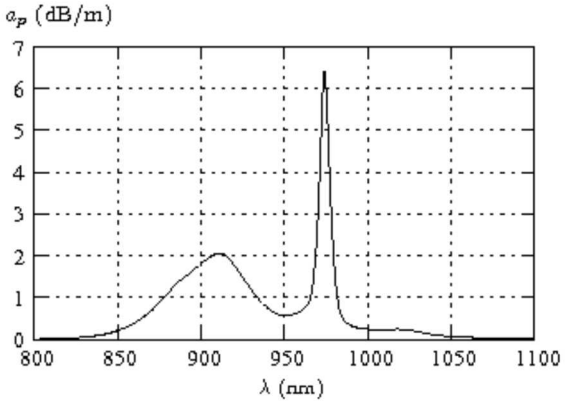

FIGURE 7

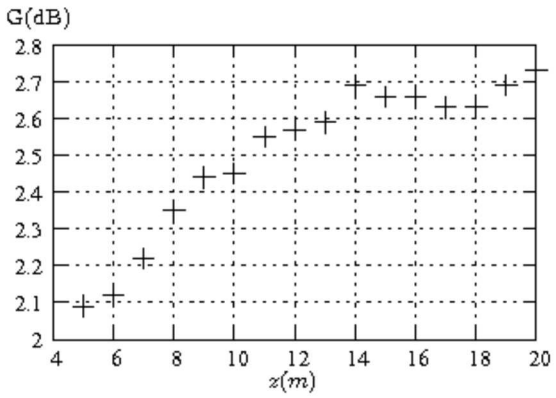

FIGURE 8